Physica C 169 (1990) 401–412
North-Holland

CRYSTAL STRUCTURE, ATOMIC ORDERING AND CHARGE LOCALIZATION IN $Pb_2Sr_2Y_{1-x}Ca_xCu_3O_{8+\delta}$ ($x=0$, $\delta=1.47$)

M. MAREZIO [1,2], A. SANTORO [3], J.J. CAPPONI [2], E.A. HEWAT [4], R.J. CAVA [1] and F. BEECH [3]

[1] *A.T.&T. Bell Laboratories, Murray Hill, NJ 07974, USA*
[2] *Laboratoire de Cristallographie, CNRS-UJF, 166X-38042 Grenoble cedex, France*
[3] *Reactor Division, NIST, Gaithersburg, MD 20899, USA*
[4] *LETI-CENG, 85X-38041 Grenoble cedex, France*

Received 15 March 1990
Revised manuscript received 22 June 1990

Neutron, X-ray and electron diffraction measurements have been carried out on $Pb_2Sr_2Y_{1-x}Ca_xCu_3O_{8+\delta}$ samples. The oxygen incorporated in the structure during the oxidation is located on the (Cu) planes sandwiched between the two (PbO) layers. A theoretical composition of $\delta=2$ is possible, although in practice only a stoichiometry corresponding to $\delta=1.9$ has been achieved so far. The extra oxygen present for $\delta>0$ forms ordered structures in which the Cu cations of the (CuO_δ) planes have square planar coordination in $Pb_2Sr_2YCu_3O_9$, either square planar, pyramidal, and octahedral, or only pyramidal coordination in $Pb_2Sr_2YCu_3O_{9.5}$, and exclusively octahedral coordination in $Pb_2Sr_2YCu_3O_{10}$. In the range of composition $0\leq\delta\leq 1$, mixtures of two phases are obtained, one with $\delta=0$ stoichiometry and the other with $\delta=1$, and whose relative quantities depend on the total amount of oxygen incorporated by the sample. The positive charges induced in $Pb_2Sr_2YCu_3O_{8+\delta}$ by oxygen incorporation oxidize the Cu^{1+} cations to 2+ and some of the Pb^{2+} cations to 4+. An order between Pb^{2+} and Pb^{4+} is established and this localization hinders the charge transfer to the conducting (CuO_2) planes and, for this reason, no superconductivity is present in oxidized samples. The cation valences are estimated from the co-ordination numbers and from the bond length-bond strength relationship.

$Pb_2Sr_2YCu_3O_8$ becomes superconducting at ≈ 80 K when some of the trivalent Y cations are replaced by divalent Ca. In this case the extra positive charges oxidize the Cu^{2+} cations in the CuO_2 planes instead of Pb^{2+} to 4+ and Cu^{1+} to 2+, as does the incorporation of oxygen. This different behavior can be explained as a concentration effect which changes the oxidation/reduction potentials. When heat treated at 500°C in O_2, $Pb_2Sr_2Y_{0.5}Ca_{0.5}Cu_3O_8$ behaves similarly to the undoped compound. The oxygen uptake suppresses the superconducting transition which is re-established by heat treating the sample at the same temperature in N_2.

1. Introduction

The superconducting series $Pb_2Sr_2Y_{1-x}Ca_xCu_3O_{8+\delta}$ was first reported by Cava et al. [1] and almost simultaneously by Subramanian et al. [2]. The structure for $\delta=0$ and $x=0$ was found to be orthorhombic, space group Cmmm, lattice parameters $a=5.393$ Å$\approx\sqrt{2}a_p$, $b=5.431$ Å$\approx\sqrt{2}a_p$, and $c=15.733$ Å (a_p being the simple perovskite parameter) and two chemical formulae per unit cell. Zandbergen et al. [3] characterized samples of $Pb_2Sr_2Y_{1-x}Ca_xCu_3O_{8+\delta}$ by electron microscopy and confirmed the structural arrangement proposed by Cava et al. [1]. Structural refinements based on powder neutron data [4] revealed that the small orthorhombic distortion is due to disordered oxygen displacements in the PbO plane. Electron diffraction patterns perpendicular to [001] showed that the crystallites are twinned by the (110) planes (see fig. 1(a)) and that, in agreement with Zandbergen et al. [3], very weak and well defined ($hk0$) diffraction spots with $h+k$ odd, which violate the C-centering, are always present. These spots define the unit cell with $a=\sqrt{2}a_p$, $b=\sqrt{2}a_p$, and indicate that the space group is primitive and the small displacements of the oxygen atoms in the PbO layers are actually somewhat ordered [5]. Fu et al. [6] who studied the isostructural compound $Pb_2Ba_2YCu_3O_8$ by electron and neutron diffraction, obtained similar results. By taking into account the reflections violating the C-centering, they determined from the neutron diffraction data that the most probable space group for

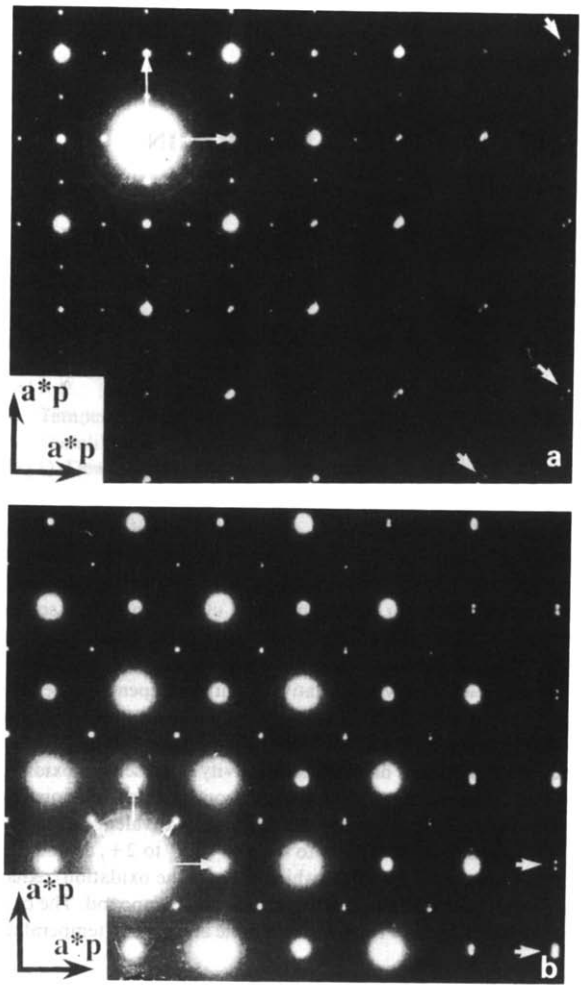

Fig. 1. (a) Electron diffraction pattern perpendicular to [001] for $Pb_2Sr_2YCu_3O_8$. Note that ($hk0$) spots with $h+k=$odd, are split. This indicates that this crystallite is twinned by the (110) plane corresponding to the (100) plane of the simple perovskite unit cell. (b) Electron diffraction pattern perpendicular to [001] for $Pb_2Sr_2YCu_3O_{9.37}$. The crystallite is twinned by the (110) plane which corresponds to the (110) plane of the simple perovskite unit cell.

$Pb_2Ba_2YCu_3O_8$ and isostructural compounds is $P22_12$.

The structure of the prototype compound $Pb_2Sr_2YCu_3O_8$ can be easily described as built of (AO) and (BO_2) layers arranged as to form either perovskite or NaCl blocks [7]. The sequence of the (AO) and (BO_2) layers for $Pb_2Sr_2YCu_3O_8$ is as follows: $(Y)_o(CuO_2)_c(SrO)_o(PbO)_c(Cu)_c(PbO)_o$-$(SrO)_o(CuO_2)_c(Y)_o$ (see fig. 2) where the subscripts o and c indicate whether the cation is at the origin or at the center of the mesh, respectively. All oxygen atoms are absent in the (Y) and the (Cu) layers. The (CuO_2)(SrO) blocks form pyramidal CuO_5 layers which represent one of the common features for most of the high-T_c copper oxide superconductors. The Sr cations are surrounded by 9 oxygens atoms arranged as the La-polyhedron in La_2CuO_4. The Y cations are surrounded by 8 oxygen atoms forming a prismatic polyhedron common to all superconducting compounds containing the (CuO_2)(M)(CuO_2) blocks in which M is either a rare-earth element or Ca. The Pb cations are sur-

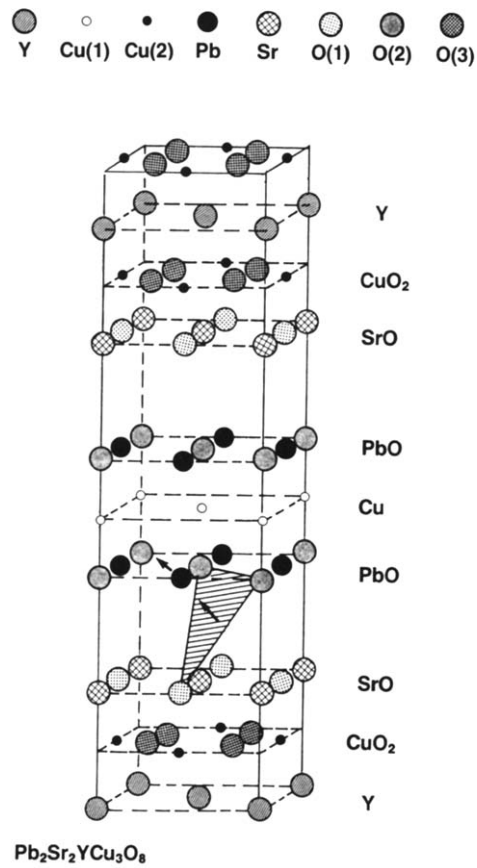

Fig. 2. Schematic representation of the structure of $Pb_2Sr_2YCu_3O_8$ viewed as a sequence of (AO) and (BO_2) layers perpendicular to the c-axis. The arrow perpendicular to the triangle of oxygen atoms indicates the direction along which the atoms are displaced, and the arrow associated with the Pb cation represents the direction along which the "lone pair" of electrons points.

rounded by 5 oxygen atoms arranged as a pyramid. However, the Pb–O distances vary over a large range with three short distances forming a triangle and two long ones (see fig. 2). This configuration is due to the "lone pair" of electrons of Pb^{2+}. The Cu cations of the oxygen-deficient (Cu) layers inserted between two (PbO) layers exhibit the stick coordination. Because of the oxygen disorder existing in the PbO layers, the stick coordination of the Cu cations may not be linear.

In $Pb_2Sr_2YCu_3O_8$ integer formal valences can be assigned to all atoms, namely Pb^{2+}, Sr^{2+}, Y^{3+}, $Cu1^{1+}$, $Cu2^{2+}$ and O^{2-}. Because of the low formal average valence for the Cu cations (1.67+), it is not surprising that $Pb_2Sr_2YCu_3O_8$ was found to be an antiferromagnetic semiconductor like $YBa_2Cu_3O_6$ and La_2CuO_4, the only difference being that its T_N is above room temperature while the latter two compounds undergo an antiferromagnetic transition below room temperature. Besides the blocks $(CuO_2)(Y)(CuO_2)$, another common feature between $Pb_2Sr_2YCu_3O_8$ and $YBa_2Cu_3O_6$ is the presence in both compounds of the oxygen deficient (Cu) layers. The semiconducting $YBa_2Cu_3O_6$ can be fully oxidized to the 90 K superconductor, $YBa_2Cu_3O_7$, and if one assumes that the anion valence is 2−, this oxygen uptake brings about an increase of 0.66+ for the average formal valence of the Cu cations (from 1.67+ to 2.33+).

As in the case of $YBa_2Cu_3O_6$, $Pb_2Sr_2YCu_3O_8$ can take up oxygen, too. This property was first discussed by Cava et al. in their original paper [1] and subsequently by Gallagher et al. [8], O'Bryan et al. [9] and Gyorgy et al. [10]. No trace of superconductivity has been detected so far in any oxidized $Pb_2Sr_2YCu_3O_{8+\delta}$ samples. In order to understand this unique behavior we have carried out thermogravimetric, X-ray, neutron and electron diffraction investigations of some oxidized samples.

2. Oxidation of $Pb_2Sr_2YCu_3O_8$

As shown in fig. 3, when $Pb_2Sr_2YCu_3O_8$ is heat treated at 450°C in O_2 atmosphere, it takes up oxygen and after about twenty hours the weight gain, as determined by thermogravimetric measurements, corresponds to $O_{9.9}$ stoichiometry. Conversely, if the same product is heat treated at 500°C in N_2 atmosphere it loses oxygen and goes back to O_8 stoichiometry [11].

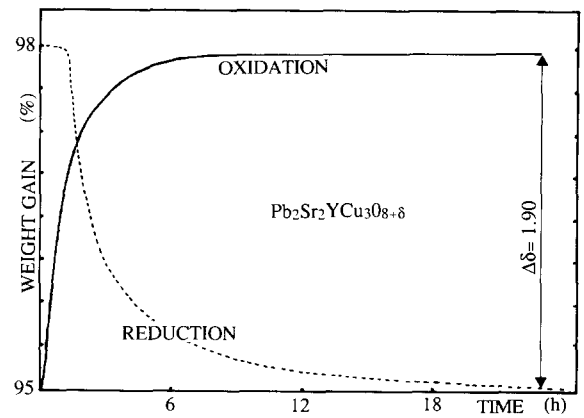

Fig. 3. Weight gain (solid line) and loss (dotted line) when $Pb_2Sr_2YCu_3O_8$ is heat-treated at 450°C in O_2 and at 500°C in N_2 temperature, respectively.

Table I
Lattice parameters for three typical samples of $Pb_2Sr_2YCu_3O_{8+\delta}$.

$\delta=0$ as prepared $a\approx b\approx\sqrt{2}\times a_p$	$\delta=1.40$, 450°C in O_2 $a\approx b\approx a_p$	$\delta=1.37$, 500°C in O_2 $a=b\approx a_p$
$a=$ 5.389(3)	$a=$ 3.838(2)	$a=$ 3.848(3)
$b=$ 5.428(3)	$b=$ 3.870(2)	$b=$ 3.848(3)
$c=$15.717(8)	$c=$15.845(8)	$c=$15.822(8)

As stated above, $Pb_2Sr_2YCu_3O_8$ is orthorhombic with cell parameters: $a\approx\sqrt{2}a_p$, $b\approx\sqrt{2}a_p$, and $c\approx 15.7$ Å. The oxidized samples are still orthorhombic; however, their unit cell changes to: $a_p\times a_p\times c\approx 15.8$ Å, space group Pmmm. The degree of orthorhombicity of the oxidized samples depends on the heat treatment temperature and the cooling rate. Table I gives the lattice parameters for three typical samples. Their values were determined by the use of a Guinier focussing camera equipped with monochromatized Fe Kα radiation and were the result of least-squares refinements. The first sample, corresponding to $\delta=0$, is orthorhombic with a unit cell $\sqrt{2}a_p\times\sqrt{2}a_p$ and $c=15.717$ Å; the second, oxidized to $\delta=1.40$ at 450°C in O_2, has an orthorhombic unit cell $a_p\times a_p$ and $c=15.845$ Å; the third sample, which was oxidized at 500°C in O_2,

corresponding to $\delta = 1.37$, has a tetragonal cell a_p and $c = 15.822$ Å. The latter sample is found to be tetragonal because the orthorhombic crystallites are twinned along the (110) plane of the sample perovskite cell (see fig. 1(b)) and the dimensions of the twin domains are of the same order of magnitude or smaller than the diffraction correlation length. Thus, the powder diffraction technique cannot detect the difference between the a- and the b-axes.

Figure 4 shows the variation as a function of δ of the c parameter for $Pb_2Sr_2YCu_3O_{8+\delta}$. It can be seen that for the interval $0 < \delta < 1$ the samples contain two phases, one corresponding to $\delta = 0$ and one to $\delta = 1$. This means that when a sample with O_8 stoichiometry begins to incorporate oxygen, domains are formed, each corresponding to one of the two stoichiometries: $Pb_2Sr_2YCu_3O_8$ or $Pb_2Sr_2YCu_3O_9$. Since the powder X-ray diffraction patterns indicate the presence of two phases the domains must be larger than the X-ray diffraction correlation length. For $\delta \geq 1$ all the (Cu) layers have the composition (CuO_δ). The samples become single-phased and the c parameter increases with increasing δ. It is worthwhile to point out that the oxidation process of $YBa_2Cu_3O_6$ produces chain fragments and is gradual, while that of $Pb_2Sr_2YCu_3O_{8+\delta}$ (for $0 < \delta \leq 1$) seems to produce blocks in which all the (Cu) layers have become (CuO).

As stated in the introduction no superconductivity has been detected so far in any oxidized $Pb_2Sr_2YCu_3O_{8+\delta}$ samples. This is quite surprising because the gain in formal valence from $Pb_2Sr_2YCu_3O_8$ to $Pb_2Sr_2YCu_3O_9$ is exactly the same as that obtained on going from $YBa_2Cu_3O_6$ to $YBa_2Cu_3O_7$. The gains are even larger if the oxidation is carried out to $O_{9.4}$ or to $O_{9.9}$. However, the oxidation/reduction potentials of the Pb^{4+}/Pb^{2+} and the Cu^{3+}/Cu^{2+} systems indicate that after the Cu^{1+} cations have been oxidized to 2+, the oxidation of the Pb^{2+} cations to 4+ should take place prior to that of the Cu^{2+} cations to 3+ (or to 2+ and one electron hole).

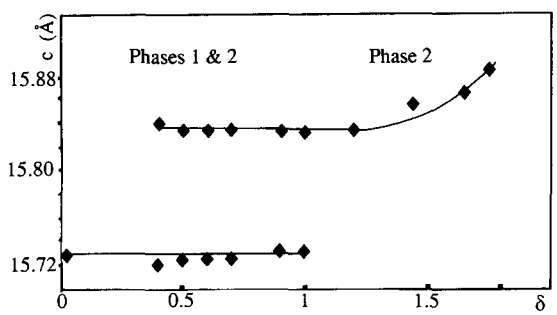

Fig. 4. Variation as function of δ of the c parameter of $Pb_2Sr_2YCu_3O_{8+\delta}$.

3. Structural refinement

The neutron powder diffraction measurements were made at room temperature with the high-resolution five-counter diffractometer at the Reactor at the Reactor of the National Institute of Standards and Technology. Neutrons of wavelengths 1.553 Å were used in the experiment with in-pile, monochromatic beam, and diffracted beam collimators having horizontal angular divergencies of 10, 20, and 10 minutes of arc, respectively. The same sample used for the determination by neutron diffraction of the $Pb_2Sr_2YCu_3O_8$ structure [4] was heat-treated at 500°C in O_2 and then cooled rapidly to room temperature. It was placed in a vanadium can of about 1 cm diameter and the data were collected in the 2θ angular range 5–120°C in steps of 0.05°.

The structure was refined with the Rietveld method [12] adapted to five-detector geometry and modified to include background parameters [13]. The neutron scattering amplitudes used in the calculations were: $b(\mathrm{Pb}) = 0.94$, $b(\mathrm{Sr}) = 0.702$, $b(\mathrm{Y}) = 0.775$, $b(\mathrm{Cu}) = 0.772$ and $b(\mathrm{O}) = 0.581 \times 10^{-12}$ cm. The peak shape could be described satisfactorily by Gaussian functions. The initial atomic parameters of the structure were those of $Pb_2Sr_2YCu_3O_8$ [5] transformed to setting of the $a_p \times a_p \times c$ cell. Since the excess oxygen was not taken into account this refinement resulted in high values of the R factors. The positional parameters of the two atoms O(3) and O(31) which form the base of the pyramid surrounding Cu(2) were highly correlated. These atoms are equivalent in the orthorhombic Cmmm space group of $Pb_2Sr_2YCu_3O_8$ and become non equivalent in the Pmmm space group of $Pb_2Sr_2YCu_3O_{8+\delta}$. In order to avoid this correlation the z parameter and the thermal factor of O(31) were constrained to be equal to those of O(3).

By analogy to $YBa_2Cu_3O_6$, the excess oxygen is likely located on the oxygen-depleted (Cu) layers, therefore, the subsequent refinements were carried out by including two additional oxygen positions, O(4) at $(0, \frac{1}{2}, \frac{1}{2})$ and O(5) at $(\frac{1}{2}, 0, \frac{1}{2})$. The starting occupancy factors for both atoms were set at 0.5. After convergence was attained, the occupancy factor of O(4) had increased to one while that of O(5) had decreased to zero, in both cases within less than one standard deviation. This indicates that part of the excess oxygen fills completely the O(4) sites at $(0, \frac{1}{2}, \frac{1}{2})$ forming infinite corner-sharing square-chains just as in $YBa_2Cu_3O_7$. The thermal factor of O(4) together with that of O(2) (located on the Pb layers) was abnormally high (24 and 19 Å^2, respectively), indicating a high degree of positional disorder for these oxygen atoms rather than true thermal vibrations. The atom O(2) was already found to exhibit a high degree of disorder in the structure of $Pb_2Sr_2YCu_3O_8$.

A difference Fourier map, obtained after the O(4) atom had been located, showed the presence of extra peaks corresponding to the position $(\frac{1}{2}, 0.22, \frac{1}{2})$. The O(5) atom was then placed in this position and introduced in the refinement. After a few cycles the wR factor decreased from 10.10 to 9.65 for an R_E of 5.26. Since there is a high correlation between the thermal and occupancy factors, in the subsequent refinements the thermal factor of O(5) was fixed at 0.95 while the occupancy factor was varied. This value was obtained in the final refinement with isotropic thermal configuration, during which the occupancy factor was fixed at the value (0.10) corresponding to the thermogravimetric analysis.

Because of the large thermal factors for most atoms, thermal anisotropy was introduced. The refinements showed that it was appreciable for Pb, Sr, Cu(1), O(1), and quite high for O(2) and O(4). For the other atoms, namely Y, Cu(2), and O(3) and consequently that of O(31), the thermal factors remained normal and in the subsequent refinements the thermal factors of these atoms were let to vary isotropically. Table II gives the final values for the positional and isotropic thermal parameters along with the occupancy factors. Table III gives the anisotropic thermal factors. It can be seen that the thermal vibrations of Pb, Sr, and Cu(1) are only slightly anisotropic. Those of Pb and Sr are similar and are high only along one direction, the b-axis, and somewhat normal along the other two. The refined B_{11} value for Sr is not significantly different from zero. The thermal anisotropy of the Cu(1) cations is low: these cations seem to vibrate (or be slightly disordered) more in the basal plane than along c. The thermal factor of O(1) is highly anisotropic along the b-axis, while it is quite normal along the a-axis. Those of atoms O(2) and O(4) are highly anisotropic as well. If these abnormally high thermal vibrations are interpreted as disorder, that of O(2) is confined in the basal plane while that of O(4) is in the ac-plane. Because of this high degree of disorder, in the subsequent refinements the atom O(2) at $00z$ was put in (xyz) and the atom O(4) in $(x, \frac{1}{2}, z)$. With this configuration the R factors did not show any significant improvement and the standard deviations of the x value for both atoms became abnormally high and of the same order of magnitude or higher than the respective differences from the special position values. The O(2) and O(4) atoms were then allowed to vary in the $(0yz)$ and $(0, \frac{1}{2}, z)$ position, respectively. The refined positional and thermal parameters for O(2) and O(4) are given in table II. It can be seen that the thermal parameters for the split atoms are reasonable except along the a-axis. The value of the O(5) occupancy factor is 0.47(3) which corresponds to a chemical formula $Pb_2Sr_2YCu_3O_{9.47}$, in good agreement with that found by thermogravimetry ($O_{9.40}$). Relevant interatomic distances are reported in table IV, those of $Pb_2Sr_2YCu_3O_8$ are listed for comparison. One unit cell of the $Pb_2Sr_2YCu_3O_{9.47}$ structure is shown in fig. 5, where the atoms are represented by their thermal ellipsoids obtained before the splitting of O(2) and O(4).

4. Description of the structure

In the structure of $Pb_2Sr_2YCu_3O_8$ the position of O(2), the oxygen atom in the PbO layer, is disordered over four positions with identical z, forming a rectangle around the average position $(00z)$ of space group Cmmm. This disorder is due to the lone pair of electrons of the Pb^{2+} cations. Two basal oxygen atoms of the pyramid surrounding Pb^{2+} move closer to the cation while the other two move farther

Table II
Refined positional, isotropic thermal (Å^2) and occupancy parameters for $Pb_2Sr_2YCu_3O_{9.47}$.

Atom	Position	x	y	z	B	n
Pb	2t mm	½	½	0.3814(2)	3.5 [1]	½
Sr	2q mm	0	0	0.2204(3)	1.5 [1]	½
Y	1a mmm	0	0	0	0.74(13)	¼
Cu(1)	1c mmm	0	0	0.5	3.5 [1]	¼
Cu(2)	2t mm	½	½	0.1027(2)	0.53(8)	½
O(1)	2t mm	½	½	0.2499(6)	5.4 [1]	½
O(2) [3]	8α 1	0	0.165(3)	0.3810(7)	5.1	½
O(3)	2r mm	0	½	0.0918(2)	0.96(8)	½
O(31)	2s mm	½	0	0.0918 [2]	0.96 [2]	½
O(4) [3]	4x m	0	½	0.458(1)	6.5	¼
O(5)	2p mm	½	0.217(8)	½	0.95 [4]	0.117(3)

[1] The thermal parameters of this atom have been refined anisotropically, the value reported in this column represents the corresponding isotropical B value.
[2] This value has been constrained to the corresponding value of O(3).
[3] These positions correspond to the refinements during which these atoms split over the positions ($0yz$) for O(2) and ($0\ \frac{1}{2}\ z$) for O(4).
[4] $B_{O(5)}$ was fixed at 0.95 (see "Structural refinement" section 3).

Table III
Anisotropical thermal parameters * (Å^2) of Pb, Sr, Cu(1), O(1), O(2), and O(4) in $Pb_2Sr_2YCu_3O_{9.47}$.

Atom	B_{11}	B_{22}	B_{33}
Pb	3.0(5)	5.4(7)	2.0(3)
Sr	−0.1(5)	2.9(6)	1.8(3)
Cu(1)	4.3(7)	3.9(7)	2.3(5)
O(1)	1.3	11(1)	4.0(5)
O(2)	5.2(9)	7(1)	2.7(6)
O(4)	15(2)	2(1)	2(1)

* For all atoms $B_{12}=B_{13}=B_{23}=0$ by symmetry.

away. It is worthwhile to mention that the Pb cation valence calculated from the Pb–O interatomic distances [14] is exactly 2+ valence units (v.u.) when this distortion is taken into account.

As shown in fig. 5 the structure of $Pb_2Sr_2YCu_3O_{9.47}$ contains more than one disordered oxygen. In addition to O(2), the incorporated O(4) of the $CuO_{1.47}$ layer and O(1) of the SrO layer, are disordered as well. This means that all of the oxygen atoms of the block (SrO)(PbO)($CuO_{1.47}$)(PbO)(SrO) are more or less displaced in a disordered fashion. During the refinements of the structure this disorder was revealed by abnormally large thermal factors. As discussed below, the disorder is larger in $Pb_2Sr_2YCu_3O_{9.47}$ than in $Pb_2Sr_2YCu_3O_8$ because of the oxidation of some Pb^{2+} to 4+. As in the case of O(2) in $Pb_2Sr_2YCu_3O_8$, the disorder of O(2) and

Table IV
Interatomic distances (Å).

	$Pb_2Sr_2YCu_3O_{9.47}$	$Pb_2Sr_2YCu_3O_8$
Pb–O(1)	2.084(8)×1	2.153(5)×1
–O(2)	2.317(7)×2	2.455(8)×1
	3.21(1)×2	2.999(7)×1
		2.322(6)×1
		3.128(6)×1
–O(4)	2.28(1)×1	
	3.19(1)×1	
–O(5)	2.17(1)×1	
Sr–O(1)	2.764(2)×4	2.740(1)×2
–O(1)		2.758(1)×2
–O(2)	2.62(1)×1	2.629(8)×1
–O(3)	2.805(4)×2	2.788(3)×4
–O(31)	2.803(2)×2	
Y–O(3)	2.416(2)×4	2.398(2)×8
–O(31)	2.413(2)×4	
Cu(1)–O(2)	1.99(1)×2	1.876(7)×2
–O(4)	2.039(7)×2	
–O(5)	2.10(1)×	
Cu(2)–O(1)	2.332(9)×1	2.285(5)×1
–O(3)	1.932(1)×2	1.927(1)×4
–O(31)	1.936(1)×2	

O(4) in $Pb_2Sr_2YCu_3O_{9.47}$ was taken into account by splitting their sites over less symmetrical positions. Since the thermal factor of O(1) was smaller than those of O(2) and O(4) and the splitting of O(1)

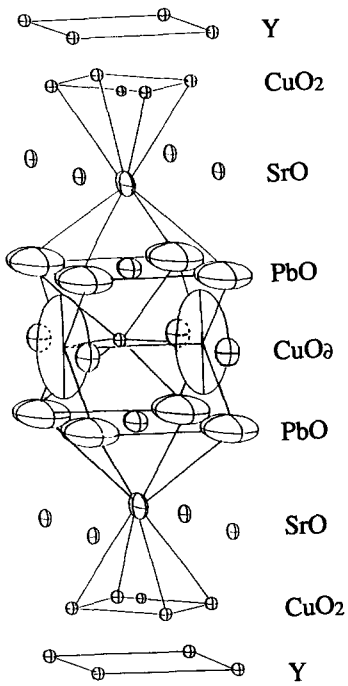

Fig. 5. One unit cell of the $Pb_2Sr_2YCu_3O_{9.47}$ structure. The atoms are represented by their thermal ellipsoids. The Pb site corresponds to that occupied by Pb^{4+} cations.

did not yield reasonable results, this oxygen atom was left in its average position with a large thermal factor. During the refinements, O(2) and O(4) moved away from their respective average positions (see table II), but no improvement was obtained for the R factors. On the contrary, for the refinement of $Pb_2Sr_2YCu_3O_8$ with split O(2) the R_w factor decreased significantly. Furthermore, the thermal factors obtained for O(2) and O(4) after their splitting were still anisotropic which strongly indicated that these oxygen atoms must also be displaced along other directions. Attempts to refine their x coordinates, however, were not successful and the atoms O(2) and O(4) were left on their average positions along the a-axis.

The oxygen incorporation up to $O_{9.47}$ induces changes in the coordination of all cations, however, only for Pb and Cu(1) these changes imply an increase in the number of the first oxygen neighbors. As in $Pb_2Sr_2YCu_3O_8$, the others cations, namely Y, Cu(2) and Sr, are surrounded by 8, 5, and 9 oxygen atoms, respectively. The variations of corresponding distances between $Pb_2Sr_2YCu_3O_8$ and $Pb_2Sr_2YCu_3O_{9.47}$ are rather small.

The calculated valences for Y and Sr, shown in table V, are smaller than their ideal values of 3+ and 2+, respectively. That of Y has been found to be smaller than 3+ in most of the cuprate superconductors and related compounds [15]. The calculated valence or Sr may increase if the disorder of O(1) is taken into account. Of the four O(1) surrounding Sr two will move closer and two will move farther away, but the increase in both strength for the former will be larger than the decrease of the latter. O(1) is also the apex of the pyramid surrounding Cu(2). By moving it away from its average position at $(\frac{1}{2}\frac{1}{2}z)$ the distance Cu(2)–O(1) should increase, the bond strength decrease, and the valence should be less than the value (2.18 v.u.) calculated without taking into account the disorder of O(1).

As stated above, the incorporation of oxygen induces an increase in the coordination number of the Pb and Cu(1) cations. These increases depend upon the ordering of the O(5) atoms whose sites have an occupation factor of 47%.

Electron diffraction photographs of oxidized $Pb_2Sr_2YCu_3O_{8+\delta}$ with $\delta \approx 1.5$ are shown in fig. 6(a) and fig. 6(b). At $(4a \times 2b)$ superstructure is visible in the former and a $(4a \times c)$ is visible in the latter. Note that in fig. 6(a) the $(h/4\ k/2\ 0)$ spots are somewhat elongated along the a-axis whereas the $(h\ k/2\ 0)$ ones have the typical round shape. In slow cooled samples where the twin domains are larger electron diffraction patterns from individual domains show the superstructure more clearly. All samples examined were inhomogenous with respect to the superstructures present. While the basic superstructure with unit cell $(4a \times 2b \times c)$ is seen in all samples, additional weak spots indicating $8a$ and $2c$ periodicity are seen in some patterns. There is also

Table V
Formal cation valences.

Pb(above E chains)	3.02	2.00
Pb(above F chains)	3.28	
Sr	1.58	1.63
Y	2.75	2.87
Cu(1)	1.91	1.28
Cu(2)	2.18	2.24

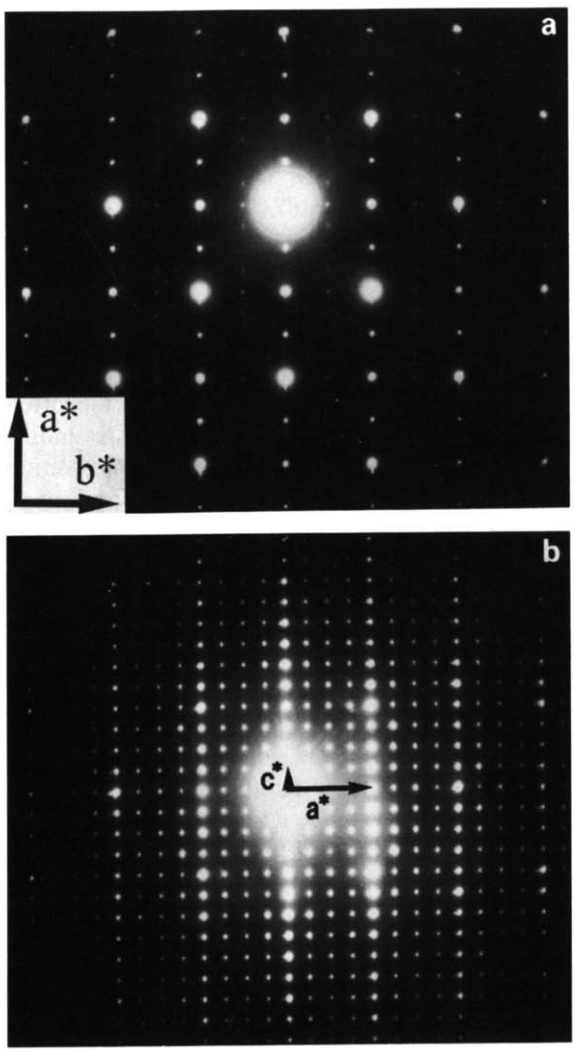

Fig. 6. (a) Electron diffraction pattern perpendicular to [001] for a $Pb_2Sr_2YCu_3O_{9.4}$ sample. A $(4a\times 2b)$ superstructure is visible. (b) Electron diffraction pattern perpendicular to [010] for a $Pb_2Sr_2YCu_3O_{9.4}$ sample. A $(4\times a)$ superstructure is visible.

considerable variation in the degree and type of ordering along the c-axis. In real space the $4\times a$ superstructure may correspond to the ordering along the a-axis of the O(5) atoms forming chains along the b-axis. Figure 7 show the (CuO_δ) layer of the $Pb_2Sr_2YCu_3O_{8+\delta}$ structure. A $4\times a$ superstructure is obtained when the full O(5) chains are ordered with the sequence FEFEF, where F and E indicate full and empty O(5) chains, respectively. The doubling of the b-axis is due to the ordering of the O(2) and O(4)

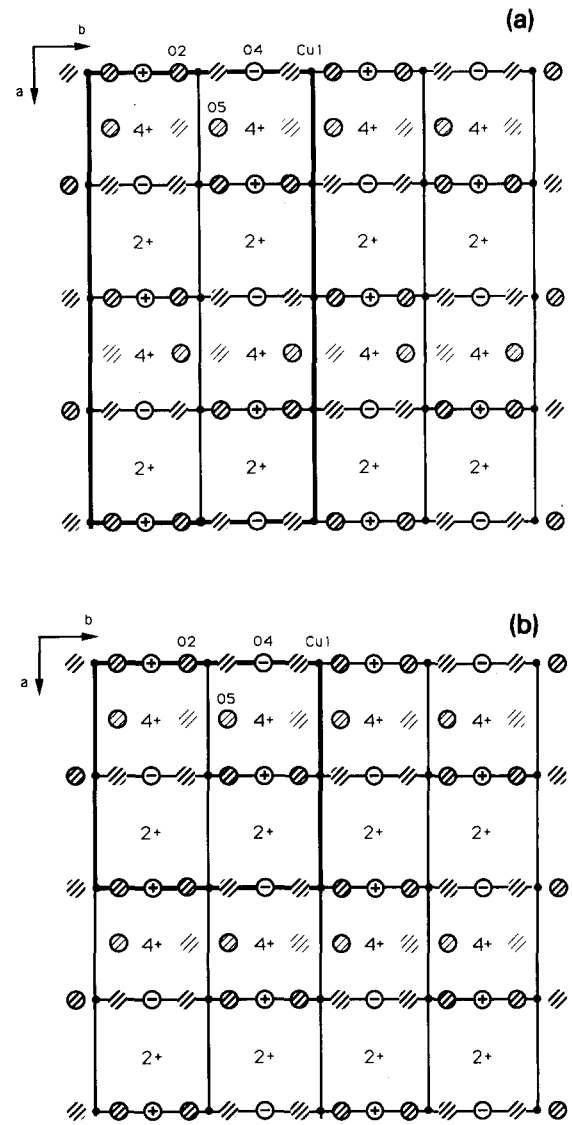

Fig. 7. (a, b) The $(CuO_{1.5})(PbO)$ layer of the $Pb_2Sr_2YCu_3O_{9.5}$ structure. The $(CuO_{1.5})$ layer comprises Cu(1), O(4) and O(5) atoms represented by small black, lightly hatched and open circles, respectively. The + and the − inside the open circles indicate the displacements along the c-axis and which site is occupied. The (PbO) layer comprises Pb and O(2) atoms, the former are represented by their probable valence and the latter by heavily hatched circles. The O(2) and O(5) atoms are split, their occupied sites are indicated by heavy circling. The $4a\times 2b$ and $2a\times 2b$ superstructures are outlined in figs. 7(a) and 7(b), respectively. Note that the occupancy of split oxygen atoms is ordered in all directions. Decorrelations would induce changes in the coordination and valence of the Pb and Cu atoms.

displacements (fig. 7(a)). The elongation of the (h/4 k/2 0) superstructure spots indicates that the full/empty ordering is not correlated in a long range fashion. This is reminiscent of the oxygen ordering found in the $YBa_2Cu_3O_{7-\delta}$ compounds for $0.4 \leq \delta \leq 0.6$. A $(2\times a)(2\times b)$ superstructure (fig. 7(b)) is obtained when the chain sequence is FEFEF and the displacements along b of the O(5) atoms are always in the same direction (positive or negative). In the FEFEF ordering all the Cu(1) cations are surrounded by oxygen pyramids (see fig. 8(a)) forming corner-sharing chains running parallel to the b-axis. Figure 8(b) shows the tilting of the pyramids resulting from the O(2) displacement along the b-axis and from that of O(4) along the c-axis.

In the FEFEF superstructure there exist two types of sites for the Pb cations. In the average structure one of these sites is seven-coordinated, above and below the empty O(5) chains, while the other is eight-coordinated (see fig. 8(a)), above and below the full O(5) chains. From the number of oxygen neighbors one can infer that the former sites are occupied by Pb^{2+} and the latter by Pb^{4+}. The cation valences calculated by the Brown and Altermatt formula and coefficients [14] are shown in table V for the structure containing the O(2) and O(4) displacements.

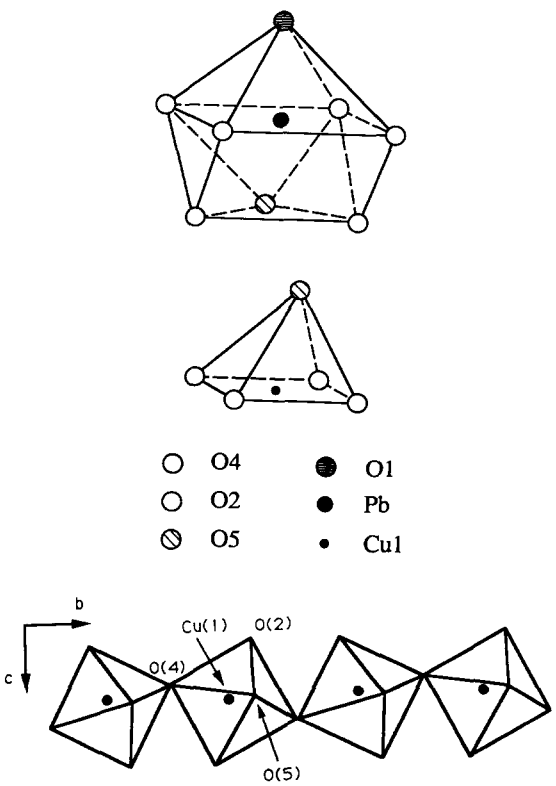

Fig. 8. (a) The Pb^{4+} coordination polyhedron (above), and the distorted pyramid surrounding Cu(1) (below). The apical oxygen is displaced of about 0.90 Å from the position above Cu(1). (b) Pyramidal chains along the c-axis. The tilting results from the O(2) and O(4) displacements along the b- and c-axes, respectively.

5. Twinning

As mentioned previously, the symmetry of $Pb_2Sr_2YCu_3O_8$ is orthorhombic Cmmm with pronounced tetragonal pseudosymmetry. Twinning by pseudo-merohedry along the (110) plane is possible and its presence has been observed in samples of this compound. The small difference between the a and the b-axes of the orthorhombic unit cell causes a slight distortion of the structure, but no structural changes occur at the twin boundary. The orthorhombic symmetry Pmmm of $Pb_2Sr_2YCu_3O_{8+\delta}$ is also pseudo-tetragonal and twinning is possible and has been observed in this compound as well. It is reasonable to believe that in this case the atomic configuration at the twin boundary is the same as that postulated for the orthorhombic phase of $YBa_2Cu_3O_{6+x}$, with all the Cu cations at the boundary in distorted tetrahedral coordination [16]. On going from $Pb_2Sr_2YCu_3O_8$ to $Pb_2Sr_2YCu_3O_9$ the unit cell changes from $\sqrt{2}a_p \times \sqrt{2}a_p \times c$ to $a_p \times a_p \times c$ and the extra oxygen atoms are incorporated along one of the axes of the second cell. This configuration, which is similar to that found in $YBa_2Cu_3O_7$, is such that the twin operation for $\delta = 1$ rotates the structure of about 90° around the c-axis, as shown in figs. 1(a) and 1(b).

For compositions in the range $1 \leq \delta \leq 1.9$ the situation on the (CuO_δ) plane is more complex. If we simply extend the model assumed for $\delta = 1$ and take into account the presence of the extra O(5) atoms, we obtain the atomic configuration shown in fig. 10. Because the O(5) atoms are shifted from their average position, a number of sites at the twin boundary would yield, if occupied, unreasonably short O–O distances. These sites, marked with a small cross in fig. 10, must be thus empty. This model may ex-

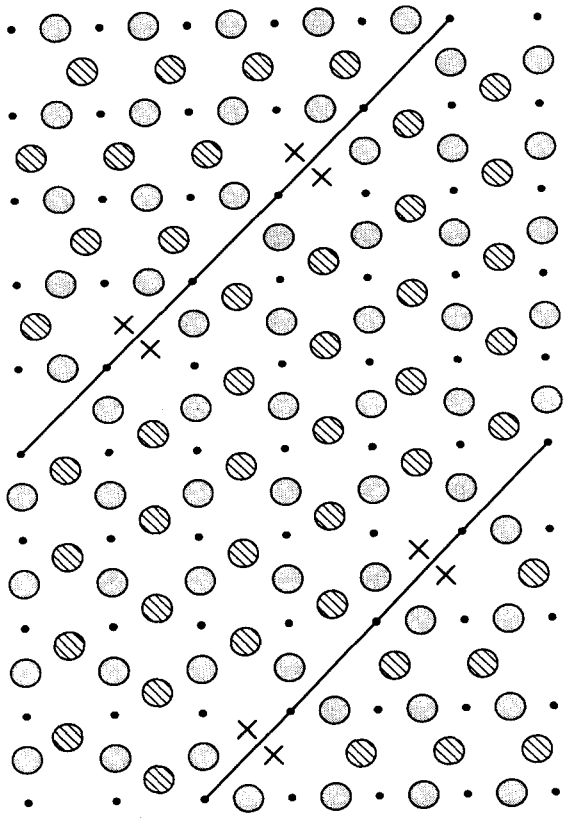

Fig. 9. Atomic configuration on the (CuO_2) layers for a composition $\delta \approx 1.9$. Dotted and hatched circles represent the O(4) and O(5) atoms and the black circles the Cu(1) cations. The oxygen atoms directly above and below each Cu are not represented for clarity. The diagonal lines are the twin boundaries and the small crosses are possible O(5) sites which are unoccupied because they would yield unreasonable O–O distances across the boundary.

plain why the composition $\delta = 2$ has never been achieved. If this interpretation is correct, the upper limit of oxygen content in this system depends on the density of the twin boundaries, that is, is a function of the preparation method and of other factors that may favor or inhibit twin formation. For example, full occupancies of sites O(4) and O(5) must induce large strains in the structure. Such strains are reduced by the occurrence of vacancies on the O(5) sublattice, which brings about the formation of twin boundaries.

The values of the interatomic distances observed in $Pb_2Sr_2YCu_3O_{9.47}$ show that it is impossible for an O(5) atom to diffuse through the gap existing between two O(4) atoms, while there is just enough room to go through two adjacent Cu atoms. These simple considerations can be used as a guide in determining possible paths for oxygen diffusion in this systems for the range of composition $1 \leq \delta \leq 1.9$. Possible models of correlated motions of the oxygen atoms, consistent with the experimental observations made so far, can be visualized (see fig. 9).

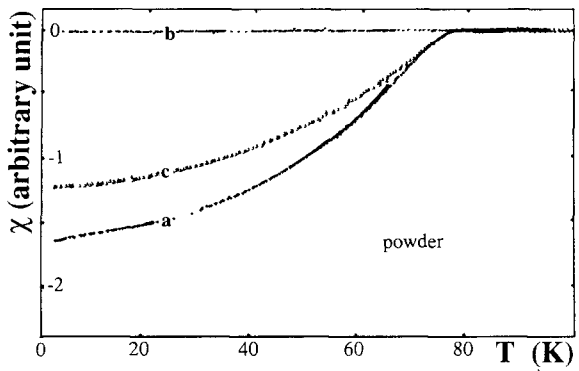

Fig. 10. AC susceptibility vs. T for a $Pb_2Sr_2Y_{0.5}Ca_{0.5}Cu_3O_{8+\delta}$ sample: with $\delta = 0$ (curve a); after oxidation in O_2, $\delta = 1.40$ (curve b); after reduction in N_2, $\delta = 0$ (curve c).

6. Discussion

The Pb cations are ordered in well defined sites which are appropriate to Pb^{2+} and Pb^{4+}. The ordered sequence can be broken if the occupied and empty O(5) sites are interchanged and, as a result, only short range ordering of the Pb cations may be present in the structure. The occurrence of this interchange may explain why the calculated Pb valences are 3.02 and 3.28 v.u. instead of the ideal 2+ and 4+, respectively. In addition, the large temperature factor of O(1) indicates possible splitting of these atoms. The displacement of O(1) from its position may take place only when this atom is bonded to a Pb^{2+}-type cation, resulting in an increase of the Pb–O(1) distance and consequent decrease of the bond strength. No splitting of O(1) would occur when this atom is bonded to a Pb^{4+}-type cation.

These results strongly corroborate the conjecture that the extra positive charges are transferred from the (CuO_δ) layers to the (PbO) ones and do not

reach the conduction layers (CuO_2). The resulting large distortions of the structure and the charge localization on the (PbO) layers, reduce mobility of the electron holes, preventing them from moving to the conduction CuO_2 layers and consequently the compound does not become a superconductor.

Cava et al. [1] showed that $Pb_2Sr_2YCu_3O_8$ becomes superconducting at about 80 K when some of the trivalent Y cations are replaced by divalent Ca. This indicates that in this case the electron holes formed on the (Y, Ca) layers are transferred to the (CuO_2) conduction layers. Figure 10 (curve a) represents the AC susceptibility versus T curve for a powder sample with the nominal $Pb_2Sr_2Y_{0.5}Ca_{0.5}Cu_3O_8$ composition. The onset of the superconductivity transition is at 78 K, however, the transition takes place over a large temperature interval and the superconducting volume is small ($\approx 20\%$). This is probably due to an inhomogeneous distribution of the Ca cations over the Y sublattice. Figure 11 represents the same type of measurements carried out on single crystal samples grown in a PbO flux and having approximately the some nominal $Pb_2Sr_2Y_{0.5}Ca_{0.5}Cu_3O_8$ composition. The onsets for single-crystal samples vary over a large temperature range (55–80 K) which indicates that the superconducting properties depend strongly upon the preparation conditions. Note that for single-crystal samples the transition ΔT's are much smaller and the estimated superconducting volumes much larger ($\approx 100\%$) than those observed for powder samples.

It has been shown that T_c has a maximum around $x=0.5$ and decreases rapidly on each side. Figure 12 shows how the AC susceptibility varies with x. For example, at $x=0.8$ only a small fraction of the sample, if any at all, becomes superconducting with an onset situated around 40 K. Therefore, the crystal whose susceptibility is shown in fig. 11 (curve a) must contain less than 50% Ca, but the amount dissolved in the sample is more homogeneously distributed than in the powder samples.

When heat-treated at 500°C in O_2 atmosphere, superconducting $Pb_2Sr_2Y_{0.5}Ca_{0.5}Cu_3O_8$ behaves similarly to $Pb_2Sr_2YCu_3O_8$. Figure 10 (curve b) shows the AC susceptibility versus T curve for a $Pb_2Sr_2Y_{0.5}Ca_{0.5}Cu_3O_8$ sample after oxidation to $O_{9.4}$ stoichiometry. As can be seen the superconducting transition is suppressed. By heat-treating this sample at 500°C in N_2 the superconducting properties are re-established (see fig. 10, curve c) and the oxygen content is reduced to O_8. This is exactly the opposite to what happens for $YBa_2Cu_3O_6$, where oxygen incorporation leads to the appearance of superconductivity.

The fact that the replacement of Y with Ca oxidizes Cu^{2+} to Cu^{3+} (or to Cu^{2+} and one electron hole) rather than Pb^{2+} to Pb^{4+} as does the incorporation of oxygen, can be viewed as a concentration effect due to the adjacency of the (Y, Ca) layers to the (CuO_2) ones. This situation changes the values of the oxidation/reduction potentials for Cu^{3+}/Cu^{2+} and Pb^{4+}/Pb^{2+}, thus the oxidation of the Cu^{2+} cations to 3+ takes place and the compound becomes

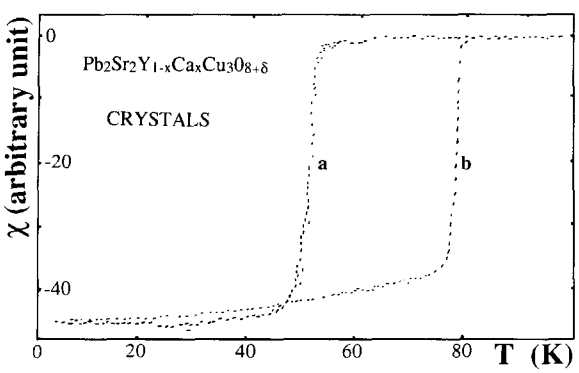

Fig. 11. AC susceptibility vs. T for two single crystals with nominal composition $Pb_2Sr_2Y_{1-x}Ca_xCu_3O_8$ with $x=0.5$ and $\delta=0$, from two different batches.

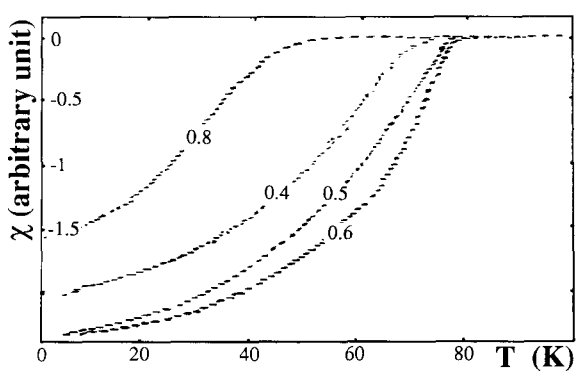

Fig. 12. AC susceptibility vs. T for $Pb_2Sr_2Y_{1-x}Ca_xCu_3O_8$ samples with different x values.

superconducting. When superconducting $Pb_2Sr_2Y_{0.5}Ca_{0.5}Cu_3O_8$ is oxygenated, the Cu^{1+} and Pb^{2+} cations of the (PbO)(Cu)(PbO) blocks are oxidized to 2+ and 4+, respectively. In order for these processes to occur, extra negative charges are needed. The unbalance is re-established by a positive charge transfer from the CuO_2 layers to the (PbO)(Cu)(PbO) blocks. This charge transfer is responsible for the suppression of superconductivity.

References

[1] R.J. Cava, B. Batlogg, J.J. Krajewski, L.W. Rupp Jr., L.F. Schneemeyer, T. Siegrist, R.B. van Dover, P. Marsh, W.W. Peck Jr., P.K. Gallagher, S.H. Glarum, J.H. Marshall, R.C. Farrow, J.V. Waszczak, R. Hull and P. Trevor, Nature 336 (1988) 211.

[2] M.A. Subramanian, J. Gopalakrishnan, C.C. Torardi, P.L. Gai, E.D. Boyes, T.R. Askew, R.B. Flippen, W.E. Farneth and A.W. Sleight, Physica C 157 (1989) 124.

[3] H.W. Zandbergen, K. Kadowaki, M.J.V. Menken, A.A. Menovsky, G. Van Tendeloo and S. Amelinckx, Physica C 158 (1989) 155.

[4] R.J. Cava, M. Marezio, J.J. Krajewski and W.F. Peck Jr., A. Santoro and F. Beech, Physica C 157 (1989) 272.

[5] E.A. Hewat, J.J. Capponi, R.J. Cava, C. Chaillout, M. Marezio and J.L. Tholence, Physica C 157 (1989) 509.

[6] W.T. Fu, H.W. Zandbergen, W.G. Haije and L.J. De Jongh, Physica C 159 (1989) 210.

[7] A. Santoro, F. Beech, M. Marezio and R.J. Cava, Physica C 156 (1988) 693.

[8] P.K. Gallagher, H.M. O'Bryan, R.J. Cava, A.C.W.P. James, D.W. Murphy, W.W. Rhodes, J.J. Krajewski, W.F. Peck Jr. and J.V. Waszczak, Chemistry of Materials 1 (1989) 277.

[9] H.M. O'Bryan and P.K. Gallagher, Chemistry of Materials 1 (1989) 526.

[10] E.M. Gyorgy, H.M. O'Bryan and P.K. Gallagher, Chemistry of Materials 1 (1989) 571.

[11] J.J. Capponi, P. Bordet, C. Chaillout, J. Chenavas, O. Chmaissem, E.A. Hewat, J.L. Hodeau, W. Korczak and M. Marezio, Physica C 162–164 (1989) 53.

[12] H.M. Rietveld, J. Appl. Crystallogr. 2 (1969) 65.

[13] E. Prince, US Tech. Note 1117, ed. F.J. Shorten, p. 8.

[14] I.D. Brown and Altermatt, Acta Crystallogr. B41 (1985) 244.

[15] R.J. Cava, A.W. Hewat, E.A. Hewat, B. Batlogg, M. Marezio, K.M. Rabe, J.J. Krajewski, W.F. Peck Jr. and L.W. Rupp Jr., Physica C 165 (1990) 419.

[16] A. Santoro, Chemistry of Superconducting Materials, ed. T.A. Vanderah (Noyes Publications), in press.